Interannual Indian Rainfall Variability and Indian Ocean Sea Surface Temperature Anomalies

Gabriel A. Vecchi

JISAO, University of Washington, Seattle, Washington

D.E. Harrison

NOAA/Pacific Marine Environmental Laboratory, Seattle, Washington

We here show that interannual variations in Indian continental rainfall during the southwest monsoon can be usefully represented by two regional rainfall indices. Indian rainfall is concentrated in two regions, each with strong mean and variance in precipitation: the Western Ghats (WG) and the Ganges-Mahanadi Basin (GB) region. Interannual variability of rainfall averaged over each of the two regions (WG and GB) is uncorrelated; however, the rainfall over these two regions together explains 90% of the interannual variance of All-India rainfall (AIR). The lack of correlation between WG and GB rainfall suggests that different mechanisms may account for their variability. During the period 1982-2001, we find very distinct relationships between Indian Ocean SST and rainfall variability over each of these two regions: warm SSTA over the western Arabian Sea at the monsoon onset is associated with increased WG rainfall (r = 0.77), while cool SSTA off of Java and Sumatra is associated with increased GB rainfall (r = -0.55). The connection between SSTA and AIR is considerably weaker, and represents the superposition of that associated with each region. We examine the robustness of the SSTA associations, and find that the relationship with WG rainfall is robust, while that with GB results from a single exceptional year.

1. INTRODUCTION

The southwest monsoon provides most of the annual rainfall in India. This monsoon exhibits non-trivial variability of precipitation over India on interannual timescales [*e.g. Shukla,* 1976; *Webster et al.,* 1998]. This variability has a profound effect on Indian economic and agricultural output, and impacts strongly the over 1 billion people in the region [*e.g. Mooley et al.,* 1981; *Parthasarathy et al.,* 1988.a; *Webster et al.* 1998]. Predicting the variability of annual rainfall over India has been a goal for the climate community for decades.

Much work on Indian continental precipitation has focused on large-scale indicators of interannual rainfall variability, often the total over India [*e.g. Shukla,* 1976; *Parthasarathy et al,.* 1988.b, 1992]. A commonly used index is the area-weighted integral of the rainfall measured by a national network of rain gauges, usually referred to as "All-India Rainfall" (AIR), records of which exist into the nineteenth century. Integrated indices of Indian continental precipitation have been found to connect with a variety of

Indian economic and agricultural indicators [*e.g. Mooley et al.*, 1981; *Parthasarathy et al.*, 1988; *Webster et al.* 1998].

Using subdivisional Indian rainfall data [*e.g. Parthasarathy et al.*, 1995], it has been established that there is considerable spatial structure to rainfall variability over India. Interannual and decadal variability, as well as long-term trends, in Indian rainfall have been found to exhibit significant spatial variability [*e.g. Parthasarathy*, 1984; *Rassmusson and Carpenter*, 1983; *Shukla* 1987; *Subbaramayya and Naidu*, 1992; *Gadgil et al.*, 1993; *Iyengar and Basak*, 1994]. Also, the relationships between Indian continental rainfall variability and large-scale climate parameters has been found to be spatially variably [*e.g. Mooley and Parsarathy*, 1983, 1984; *Parthasarathy and Pant*, 1984; *Mooley at al.* 1986; *Parthasarathy et al.* 1990, 1991].

We here show that interannual variability of total Indian rainfall can be described effectively using indices of variability over two distinct regions. The time series of averages over the regions are uncorrelated to each other. Their sum explains a large fraction of All-India rainfall variability – 90% of the variance over the past 23 years. The first region encompasses the Western Ghats coastal region and the other the Ganges and Mahanadi River Basins. That rainfall anomalies over the two regions are uncorrelated suggests that different processes may account for the interannual variability of precipitation in each region. We find significant and distinct simultaneous and leading sea surface temperature anomaly (SSTA) patterns associated with each regional index. However, we are unable to find similarly large-scale connections to All-India Rainfall.

In the following Section we describe the datasets used in this analysis. In Section 3 we present our parsing of Indian precipitation into the two regional Indices. In Section 4 we describe the correlations between the regional precipitation indices and Indian Ocean SSTA. Section 5 offers a summary of the results and discussion of their implications.

2. DATA AND METHODS

We use the Reynolds/NCEP Version 2 weekly 1°×1° optimally interpolated SST product [*Reynolds and Smith*, 1994; *Reynolds et al.*, 2002]. A monthly climatology of SST was generated by averaging, 1982 through 2001; anomalies were computed from this monthly climatology. Though EOF-based reconstructions of SST extending to the beginning of the century are available, we restrict our analysis of SSTs to the 20-year period 1982-2001, because from 1982 onwards there is a relative homogeneity of the data sources (satellites and in situ) and the analysis techniques for the gridded dataset.

We use the pentad CPC Merged Analysis of Precipitation (CMAP) on a global 2.5°x2.5° grid, which combines satellite estimates of precipitation with in situ rain gauge measurements [*Xie and Arkin*, 1996, 1997; available online from

NOAA/CIRES/CDC at http://cdc.noaa.gov/]. Two monthly climatologies of precipitation were generated by averaging, based on the years 1979 through 2001, and 1982 through 2001; anomalies were computed from these monthly climatologies. Each climatology is applied depending on the time-period being considered; for example, in analyses spanning 1979-2001, the 1979 through 2001 climatology was used.

We remove the trend and long-term mean from SST and precipitation anomaly data prior to our analysis. The trends are significant, over the period 1982-2001 SSTA warmed by an average of 0.2-0.6°C over most of the Indian Ocean (except for the southwest Indian Ocean, which cooled by 0.2-0.4°C); these trends represent between 50% and 250% of the local standard deviation of monthly mean SSTA. The trends in Indian precipitation are more modest, with a general tendency for drying of 0.2-0.8 mm day-1 for the 20 year period (1982-2001); these trends represent 20%-60% of the standard deviation of the local monthly mean precipitation anomaly. The inclusion or removal of the trends impacts our principal results only in detail, and not in substance.

To confirm the robustness of our analysis of the spatial structure of Indian rainfall we use rain gauge-based datasets with a considerably longer record than that of CMAP. We use a global gridded rain gauge-based, land precipitation dataset [*Hulme*, 1992, 1994; *Hulme et al*., 1998; data are available online from Dr. Mike Hulme at http://www.cru.uea.ac.uk/~mikeh/datasets/global/), on a monthly, 5° by 5° grid, from 1900 through 1998. We also make use of the seasonal 1871-2000 rain-gauge based subdivisional Indian rainfall dataset produced at the Indian Institute of Tropical Meteorology by Dr. B. Parthasarathy [*Parthasarathy et al.*, 1995; data is available online at http://grads.iges.org/india/partha.subdiv.html].

3. STRUCTURE OF INDIAN RAINFALL

We performed a grid-box by grid-box analysis of the CMAP precipitation anomalies of Indian precipitation, and found that it is dominated by two regions of high mean and interannual variance in southwest monsoon (June-September) precipitation. We develop two regional-average indices, and find that they are uncorrelated to each other. Their sum is correlated with All-India Rainfall (AIR) at 0.95 over the period 1979-2001, and at 0.88 over the period 1900-1998.

Figure 1 shows maps of the mean (Fig. 1.a) and the standard deviation (Fig. 1.b,.c) of the monthly mean anomalies of SW monsoon land precipitation anomalies from the CMAP dataset. In each panel of Figure 1 we indicate the two regions which will be used to generate precipitation indices. Figure 1.c shows the actual grid cells that are used to construct the land precipitation indices. There are two primary regions of strong precipitation and strong precipitation variability: the Western Ghats, and the Ganges and

Mahanadi River Basins. The Western Ghats have the strongest mean and variability in precipitation, concentrated along the coast west of the Western Ghat Mountains. The Ganges-Mahanadi Basin has strong mean and variability extending inland from the Bay of Bengal.

To explore relationships between the two regions we compute the correlation between mean SW monsoon anomaly at each CMAP grid box in South Asia and the precipitation anomaly at points in each region, examples are shown in Figure 2.a-.b. The mean SW monsoon precipitation anomaly for points within each region is significantly correlated (at the 95% level) with that of the other points within the region, but not between the regions. Because the precipitation variability is locally coherent in each region, it is sensible to define regional precipitation indices. The Western Ghats Index (WGI) is defined as the spatial average of continental precipitation anomaly in the region (72.5°E-77.5°E, 7.5°N-20°N), and the Ganges-Mahanadi Basin Index (GBI) is defined as the spatially averaged continental precipitation anomaly over the region (77.5°E-87.5°E, 20°N-27.5°N). We define our All-India Rainfall Index as the precipitation anomaly averaged over all the grid cells shown in Figure 1.c.

Figure 3.a shows time series of the mean WGI and GBI during the SW monsoon. The two indices are not correlated; for the 23-year period, 1979-2001, the correlation coefficient between the two regional indices is 0.2, which is not statistically significant even at the 85% level. Further, if the year 1980 is removed from the analysis, the correlation between the two time series is 0.08; thus the small nominally-positive correlation between the two time series arises principally from one extreme year. Each regional index is significantly and positively correlated with AIRI; the correlation between WGI and AIRI is 0.76 and between GBI and AIRI it is 0.72.

Figure 3.b shows time series of the AIRI and of the average of the two regional indices (i.e. 0.5*[GBI+WGI]). The average of the two regional indices is very strongly correlated with AIRI (0.95). The sum of these two independent regional indices explains 90% of the interannual variance of Indian subcontinent precipitation in the CMAP precipitation dataset. We note that moderate changes in the definition of the regions used to compute the indices affects only the details of the results.

As can be seen in Figure 3, extrema in All-India rainfall result sometimes from one index or the other, and sometimes by a combination of the two. For example, the years 1984-86 showed negative precipitation over All-India; however, all of India wasn't dry: while the Western Ghats were extremely dry, the Ganges-Mahanadi Basin was close to normal. In 1988, All-India indicates a wetter than normal year, which is made up principally of enhanced precipitation over the Western Ghats; the Ganges-Mahanadi Basin was dryer than normal. In 1994 the All-India signal is dominated by the ex-

treme precipitation anomaly in the Ganges-Mahanadi Basin. The converse occurs in 1997-8, which was wetter in the Western Ghats but near-normal in the Ganges-Mahanadi Basin. And sometimes the precipitation anomalies in both regions are in phase, such as 1980-1981 (wet), 1986-1987 (dry) and 2000 (dry).

The CMAP dataset is based on both satellite and rain gauge estimates of precipitation, and thus spans only the period 1979-present. To confirm that the results based on the recent decades were evident in the past century, we used the Hulme gridded precipitation (HGP) dataset over the period 1900-1998. Again, we found that there are two variance and mean precipitation maxima in the Indian sub-continent, corresponding well with those found in CMAP. Further, the correlation coefficient between the two regional indices (defined as above, but computed using the HGP data) is 0.15, which is not statistically significant at the 90% level, and the correlation of the average of the two indices with AIRI is 0.88. Thus, over the entire 20th century the two regional indices are uncorrelated, and explain a large part of the variance of AIRI.

Similar relationships are found in the sub-divisional Indian rainfall data of Parthasarathy *et al*. [1995] over the period 1871-2000. There are two peaks in JJAS rainfall and rainfall variability, one in the Western Ghats and the other in the Ganges-Mahanadi Basin. We generate indices for the Western Ghats and Ganges-Mahanadi Basin regions. The sub-divisional rainfall WGI is computed as the area-weighted sum of rainfall in: Konkan; Madhya Mharashtra; Marathawada; Coastal, Northern Interion and Southern Interior Karnataka; and Kerala sub-divisions. The sub-divisional rainfall GBI is computed as the area-weighted sum of rainfall in: Orissa, Bihar Plateau, Bihar Plains, East Uttar Pradesh and East Madhya Pradesh sub-divisions. The correlation between the two regional indices over the period 1871-2000 is not significant ($r = 0.04$); while together they are strongly correlated to All-India rainfall ($r = 0.91$). Thus, it appears that the relationship found in recent decades using the merged satellite/rain gauge dataset is a characteristic of the interannual rainfall variability over India.

4. SSTA/RAINFALL CORRELATIONS

In this section we describe the correlations between Indian Ocean SSTA and WGI, GBI and All-India Rainfall, using the rainfall indices based on the CMAP precipitation dataset. We have found strong simultaneous and leading correlation patterns with each regional index; there are even statistically significant correlation patterns between SW monsoon precipitation anomalies and Indian Ocean SSTA during the preceding NE monsoon. The correlation patters for each region are notably different. We find no similarly strong connections between AIRI and Indian Ocean SSTA

using the same methods. Thus, using SSTA to help forecast precipitation variability in each region independently appears to provide a better tool for forecasts of seasonal precipitation over the Indian subcontinent than does focusing on All-India rainfall. We note that the character of the SSTA correlation features is largely the same when computed using rainfall indices computed with the 1982-2000 subdivision rainfall [*Parthasarathy et al.*, 1995], and differ only in magnitude.

Figure 4 shows the correlations of GBI and WGI, respectively, precipitation anomaly during JJAS and Indian Ocean SSTA in different two-month averages, starting from the June-July (JJ) at lag zero (Figure 4.a, 4.e) and moving back in time to the September-October (SO) preceding the southwest monsoon (Figure 4.d, 4.h). Only correlations greater than 0.4 (statistically significant at roughly the 92.5% level, assuming a Normal distribution and that each year is an independent sample); only correlations in areas where the standard deviation of SSTA exceeds 0.3°C are shown (assuming a Normal distribution, if the standard deviation is less than 0.3°C, one expects less than 10% of the samples to have an amplitude exceeding 0.5°C).

Figure 4.a shows that moderate simultaneous correlations between GBI and cold SSTA off the coasts of Sumatra and Java exist (peak values <0.6). These correlations are evident from the beginning of the SW monsoon, but disappear following that. In the inter-monsoon period there are scattered associations of enhanced GBI with cold SSTA in the southeastern Indian Ocean (Figure 4.b). There are more extensive correlations with southern Indian Ocean cold SSTA in the preceding NE monsoon (Figure 4.c). The correlations between enhanced SW monsoon GBI and enhanced cold southern Indian Ocean SSTA in the preceding SW to NE inter-monsoon period (Figure 4.d) are stronger and more extensive than any of the instantaneous correlations (Figure 4.a). These correlations exceed 0.5 over a large area and can exceed 0.7 locally.

We note that in the correlations between JJ SSTA and JJAS CMAP-based GBI there is an area of negative correlation in the northern Arabian Sea which is just below the threshold for significance, with values between 0.3-0.4. When the SSTA correlations are computed using the GBI based on the sub-divisional Indian rainfall this area of negative correlation exceeds the significance threshold of 0.4. As the SST record lengthens this relationship should be revisited.

Figure 4.e shows a strong simultaneous correlation between WGI and warm SSTA in the western Arabian Sea. This correlation exceeds 0.7 over a large area. There is also correlation with warm SSTA in the southwestern Indian Ocean, south of the Bay of Bengal and in the South China Sea, though of more moderate amplitudes. Relatively strong positive correlations are evident at the beginning of the southwest monsoon in the western Arabian Sea (MJ), but

not prior to that. However, the southern hemisphere correlations continue through the inter-monsoon period (Figure 4.f) and strengthen during the NE monsoon preceding the enhanced precipitation. In fact, in DJ they exceed 0.6 in the southwest Indian Ocean, and locally exceed 0.7 (Figure 4.g). Prior to DJ the southern hemisphere correlations are smaller and not significant (Figure 4.h). In SO prior to the enhanced WG precipitation there are cold SSTA connections in the western Pacific Ocean, and warm SSTA connections over the eastern Arabian Sea.

To determine whether the statistically significant patterns of correlation we find are representative of the entire 20-year record or whether they result from extrema in the record we examine more carefully the three principal correlation patterns for each precipitation index. For the GBI we explore the June-July Sumatra/Java, and the December-January and September-October southern Indian Ocean signals. For the WGI we explore the June-July Western Arabian Sea, the March-April central south Indian Ocean and the December-January western south Indian Ocean signals.

Figures 5 and 6 show scatter plots of each SSTA index with the corresponding JJAS precipitation Index, each panel shows the correlation coefficient. Only for the June-July Sumatra/Java SSTA index correlation with GBI (Figure 5.a) does the removal of an outlier fundamentally change the correlation coefficient; in the absence of the extreme value in 1994 the correlation coefficient drops from –0.55 to –0.21; thus, the relationship between June-July Sumatra/Java SSTA and JJAS GBI is not robust. However, for all other SSTA indices, the relationship appears to be robust. The strongest correlation coefficient is that between western Arabian SSTA and WGI at 0.77 (Figure 6.a).

We explore the correlations of Indian Ocean SSTA to All-India precipitation in Figure 7; we shade those values whose amplitude exceeds 0.4 and whose local standard deviation of SSTA exceeds 0.3°C, and we contour without shading those correlations which are not significant but whose local standard deviation of SSTA exceeds 0.3°C. Notice first that for none of the month-pairs are there large-scale areas of significant correlation akin to those evident in the regional index correlations (Figure 4). Also, in all the months, the correlation patterns are a superposition of the WGI and GBI correlation patters, with reduced amplitude; this is to be expected since GBI and WGI are uncorrelated and their sum represents a large part of the variance of AIRI.

Starting in DJ through the beginning of the SW monsoon (Figure 7.a-.c) there is an indication of an east-west SST dipole associated with AIRI, whose poles have limited – if any – statistical significance. However, the dipole pattern arises from two independent correlation patterns and does not represent a single dipole mode. The positive correlations in the western part of the basin arise from the WGI contribution to AIRI, while the negative correlations in the

eastern part of the basin arise from the GBI contribution to AIRI.

5. DISCUSSION

On interannual time scale there are two distinct regions of Indian continental summer rainfall, which we have labeled "Western Ghats" and "Ganges-Mahanadi Basin". Over the two decades of satellite data used here, and over 130 years using land station data, the two regional-average time series of rainfall, WGI and GBI, are uncorrelated at 90%. Further the sum of the two time series accounts between 80-90% of the interannual variability of rainfall averaged over all of India, using "All-India" rainfall indices. To a very useful degree then, these two regions may be used to study interannual rainfall variability of total rainfall over India.

A commonly used alternative method for decomposing the variability of a geophysical field is Empirical Orthogonal Function (EOF) analysis. We performed an EOF analysis of the twenty year record of rainfall, which produces substantially the same result as other EOF analysis of regional Indian precipitation anomalies [*e.g. Rassmusson and Carpenter*, 1983; *Shukla*, 1987]. The EOFs indicate that there are two principal modes of variability: a continent-wide "breathing" mode (~30% of the variance) and a dipole-like mode (where the Ganges-Mahanadi Basin varies inversely with the Western Ghats; ~11% of the variance). On the surface, the EOF description of the modes of precipitation variability over India appears to differ with our two-region decomposition. However, these EOFs are the expected statistical descriptions for a system whose principal dynamical modes are two independently varying centers of strong variance [*Domenget and Latif*, 2002]. Thus, despite the apparent dissimilarity, the EOF description is consistent with our result that Indian precipitation is made up primarily of two independently varying centers of action.

Our result also at first appears to contradict previous work that has described widespread correlation of net summer rainfall over India. Hastenrath [1987, Figure 3] shows that the correlation coefficient between summer mean local precipitation anomalies and the All-India Rainfall total is positive throughout India. Goswami *et al.* [1999], using the same precipitation dataset we have used (but with fewer years), find that the precipitation anomaly at all points in an extended Indian monsoon region is positively correlated with the average over the entire region. Goswami *et al.* [1999], argue that the interannual variability of precipitation of the Indian monsoon is largely spatially coherent because "positive correlations over the entire… region establishes that the interannual variability of the seasonal summer mean precipitation variability is indeed coherent over the… region" [*Goswami et al.*, 1999, p 615].

However, it does not follow, from modest widespread lo-

cal correlation with a large-scale average, that there is widespread coherence between individual locations. Our results provide a clear counterexample. While it is true that both the Western Ghats and Ganges-Mahanadi Basin time series are correlated with All-India rainfall, it is also true that these two time series are uncorrelated to each other. Thus, there is no inconsistency between our description of the system and the results of Hastenrath [1987] and Goswami *et al.* [1999].

Recognition of the independence of the summer averages of these two primary regions of Indian rainfall invites a new perspective, one in which it is not surprising that there are different useful statistical relationships between large scale environmental conditions and the individual regional time series. It appears likely that different mechanisms may be responsible for the interannual variability of precipitation in each of the two regions.

In hindsight, this result is not altogether unexpected: India is a very large country with orographic features that divide it, and the moisture pathways to each of the two regions are different. During the SW Monsoon, there is strong moisture transport onto India and the rest of southern Asia, some of which is picked up by evaporation from the surrounding waters (the Arabian Sea and Bay of Bengal) and some of which is transported from the southern Hemisphere [*e.g. Findlater,* 1969; *Saha*, 1970.b; *Cadet and Greco*, 1987.a,b]. The moisture flux across the west coast of India over the Arabian Sea is a principal source of the precipitation over the Western Ghat Mountains, often resulting from periods of heavy orgraphically forced rainfall [*e.g. Saha and Bavadekar*, 1977; *Rakhecha and Pisharoty*, 1996]. Meanwhile the rainfall over the Ganges-Mahanadi River Basins is associated with tropical depressions formed over the Bay of Bengal which propagate northwestward onto continental India, and whose effect is principally limited to the Ganges-Mahanadi River Basins [*e.g. Murakami*, 1976; *Rakhecha and Pisharoty*, 1996]. Thus, the rain that falls in the two regions, Ganges-Mahanadi Basin and Western Ghats, results from different synoptic circulation structures and is also liable to be directly influenced by two different adjacent seas, the Bay of Bengal and the Arabian Sea respectively.

We have described a strong positive correlation, at the onset of the monsoon, between Arabian SST anomaly and WGI in the months preceding the onset of the summer monsoon. The robustness of this correlation (Section 4) encourages its use in short term forecasting of the coming SW monsoon net rainfall over the Western Ghats. Others have noted a relationship between Indian continental rainfall and SST in the Arabian Sea. Saha [1970.a, 1974] suggested that the SST in the Arabian Sea could be an important aspect of the monsoon circulation and its rainfall over India. Many data analysis studies have found that the SW monsoon Indian rainfall is positively correlated to the SSTs in the

Arabian Sea, with the correlation being strongest with western India precipitation [*e.g. Shukla and Misra*, 1977; *Joseph and Pillai*, 1984; *Rao and Goswami*, 1988; *Ramesh Kumar and Sastry*, 1990]. Modeling studies [*e.g. Shukla*, 1975; *Druyan et al.*, 1983; *Krenshaw*, 1988; *Alapathy et al.*, 1995] have found that Arabian Sea SST anomalies influence monsoon circulation and rainfall over India, and have identified mechanisms for the connection. Increased Arabian Sea SSTs are associated with enhanced evaporation and atmospheric circulation, which increases rainfall in the western part of India. In this perspective, the factors that control SST anomalies in the Arabian Sea also significantly affect the net summer rainfall over the Western Ghats (and a significant component of All-India Rainfall).

Our analysis also identifies statistically significant zero-lag negative correlation between SSTA in the Java-Sumatra region and GBI (Section 3). This zero lag result is not at all robust; it results primarily from a single year (1994) with very large SST and rainfall anomalies. We note that there is an area of borderline significance in the northern Arabian Sea which exhibits negative correlation between JJ SSTA and GBI, this relationship crosses the threshold for significance when the sub-divisional rainfall dataset is used for an index. We suggest that, as the record lengthens, this relationship be re-examined.

We also found statistically significant positive correlations with WGI (and negative correlations with GBI) and SSTA leading the onset of the southwest monsoon by up to nine months (Figure 4). The relationships are relatively robust, although less strongly so than the zero lag western Arabian Sea connection to WGI (Figures 5, 6). No simple ideas have occurred to us to rationalize these patterns, and it is puzzling that the lead relationships of six and nine months with GBI should be stronger than the simultaneous correlations. However, since these correlations are both significant and relatively robust they may be useful in SW monsoon rainfall forecasts. Data and modeling studies should be pursued to understand the mechanisms behind these observed relationships.

Somewhat to our surprise, we find no correlations were found between GBI and Bay of Bengal SST anomalies. Most of the synoptic systems that bring rainfall to that part of India originate over the Bay of Bengal, and there is a strong relationship between Bay of Bengal SST and subseasonal monsoon breaks [*Vecchi and Harrison*, 2002]. While it is possible that there is, in fact, no systematic interannual relationship between Bay of Bengal SST and GBI rainfall, it is also possible that this lack of correlation on interannual timescales arises from the fact that the Bay of Bengal is particularly poorly sampled for SST over much of the year [*e.g. Reynolds and Smith*, 1994; *Reynolds et al.*, 2002]. On subseasonal timescales, the widely used NCEP SST analysis seriously underestimates the SSTA variability in the Bay of Bengal during the southwest monsoon [*e.g. Premkumar et*

al., 2000; *Sengupta and Ravichandran*, 2001; *Vecchi and Harrison*, 2002]. Thus, it is possible that interannual SST variations in the Bay of Bengal are also poorly represented in the NCEP SST product. Aliasing of the large amplitude (1-2°C) subseasonal variability could alone easily impact the utility of this product for low frequency climate studies. We do not wish to single out the NCEP SST analysis for concern here; any modern blended SST analysis that depends on infrared satellite as well as in situ data will be limited in this region.

We also looked for relationships between Indian Ocean SST and the first two principal components (EOFs) of Indian rainfall, and between All-India Rainfall. In neither case were we able to find large scale SST anomaly patterns with significant correlation at the 92.5% level. Relative to AIRI, we find correlation patterns consistent with the union of our WGI and GBI results, but the correlations fail to reach our 92.5% significance threshold over a large area. Interestingly, the structure of the non-significant correlation between AIRI and Indian Ocean SST between December-January and June-July is reminiscent of the recently identified Indian Ocean Dipole or Zonal Mode [*Saji et al*., 1999; *Webster et al*., 1999]. However, this pattern arises because each of the two uncorrelated components of AIRI (GBI and WGI) is associated with a different pattern in SSTA (cold SST in the east, warm SST in the west, respectively). This suggests caution in interpreting relationships between the IODM and AIRI.

Other relationships between AIRI and Indian Ocean SST, besides the Arabian Sea connections, have been found. We do not wish to do a comprehensive summary, but offer some examples of relationships described in the literature. Nicholls [1995] finds that AIRI is correlated positively to April SSTA in the Australia/Indonesia region. Sadhuram *et al*. [1997] find significant positive correlation between November-December SSTA in the eastern equatorial Indian Ocean and AIRI. Goswami *et al*. [1999], defining a "broad-scale circulation index" for the Indian monsoon, find significant positive correlations with southern Indian Ocean SSTA. In an extensive analysis of the relationship between Indian Ocean SSTA and AIRI, Clark *et al*. [2000] finds significant correlation between AIRI and SSTA in a variety of locations in India; these include positive correlations between the eastern Arabian Sea and central Indian Ocean in September-November (for the years 1977-1995), the northern Arabian Sea and Indian Ocean northwest of Australia in December-February (for the years 1945-1995).

From this brief summary, and the results presented in this paper, it is evident that a wide range of somewhat conflicting results have been described between Indian Ocean SST anomalies and Indian continental rainfall anomalies. Every study finds one or more correlations (although few discuss the robustness of their correlations) but the relationships often involve different regions at different leads. We believe

that this uncomfortable situation may partly arise because of uncertainties in our knowledge of Indian Ocean SST.

A specific example usefully illustrates the present situation. Clark *et al.* [2000] have recently described an SST anomaly pattern that leads All-India rainfall by 9 months. They worked with roughly the same time period that we have used here, but used an early version of the Hadley Centre SST analysis instead of the NCEP SST analysis that we used. We are unable to reproduce their result using NCEP SST, even when we use a rain gauge-based All-India Rainfall index. The region in which Clark *et al.* [2000] found correlation has very small SST anomaly variance, further, there is strong variability on subseasonal timescales in the SST in that region [*e.g. Harrison and Vecchi*, 2001; *Vecchi and Harrison*, 2002]; the SST analysis 'signal to noise' is large there. It is possible that the large relative uncertainties associated with the SSTA in this region are responsible for the different reported SSTA/AIRI relationships.

Much of the Indian Ocean is not well observed during various periods of the year, either by infrared satellites or by ships and drifting buoys [*e.g. Reynolds and Smith*, 1994; *Reynolds et al.*, 2002]. Harrison and Vecchi [2001] and Vecchi and Harrison [2002] discuss some aspects of how different the Indian Ocean SST variability appears to be when it is observed via the TRMM Microwave Imager rather than the NCEP weekly SST analysis. In the presence of significant persistent cloud, storminess and high winds, there typically is little data available for the preparation of fields of SST. It is possible that our entire view of Indian Ocean SST will change as we accumulate multi-decadal microwave SST information. We note that the international climate community is working to improve the in situ Indian Ocean observing system [*e.g. Smith and Koblinsky*, 2001]. Sustained deployments of surface drifters and moorings in the region should substantially improve SST analysis products.

While we are on the topic of limitations in this study, we wish to acknowledge that use of only the most recent 20 years of data may affect our SSTA correlation results. Many studies have noted that statistical relations can be different in these modern decades than they were in earlier decades [*e.g. Hastenrath*, 1987; *Torrence and Webster*, 1999; *Clark et al.*, 2000; *Krishnamurthy and Goswami*, 2000]. But it is only over these recent decades that relatively homogeneous (in the sense that they were produced from similar sensors and consistent analyses) and complete SST and precipitation data sets are available. As the satellite data records increase in duration, all of these relationships should be revisited.

We have not so far commented on the effects of the El Niño-Southern Oscillation (ENSO) phenomenon on WGI and GBI. Considerable work has been done connecting All-India Rainfall to ENSO. A connection has been found between deficient rainfall in India in the SW monsoon and El Niño conditions [*e.g. Rassmusson and Carpenter*, 1983;

Mooley and Parthasarathy, 1983, 1984; *Yu and Slingo*, 1995]. This relationship is not robust, however, with the major 1997-8 El Niño standing as a notable exception; nor is it stationary, there have been interdecadal changes in the relationship [*e.g. Torrence and Webster* 1999, *Krishnamurthy and Goswami* 2000].

We have computed correlations between AIRI, WGI and GBI and two commonly used El Niño SSTA indices (NIÑO3 – SSTA averaged 150°W-90°W, 5°S-5°N; NIÑO3.4 – SSTA averaged 170°E-125°W, 5°S-5°N). With our chosen data sets and over our analysis period, we find no significant correlation between the CMAP-based All-India Rainfall Index and NIÑO3 or NIÑO3.4 SSTA, at any lag between –25 and 25 months. There modest correlation (r = 0.42) between GBI and NIÑO3.4, with GBI leading NIÑO3.4 by ~4 months, but this correlation is due principally to 1994 and is thus not robust. However, we are able to find significant lead correlations between El Niño SSTA indices and WGI (r = 0.43 with NIÑO3, r up to 0.6 with NIÑO3.4), with equatorial Pacific SSTs leading WGI by 15-20 months.

That Indian rainfall can be parsed into two uncorrelated regions of high variability suggests that there are distinct mechanisms controlling the variability on interannual timescales in each region, whose superposition controls most of the rainfall over all of India. The potential utility of this new parsing of the system is evident in our SSTA correlation analysis over the Indian Ocean, in which the correlations between each region were distinct and more significant than any found with AIRI. The utility of these correlations for forecasts of monsoon precipitation over India should be investigated. We suggest that the environmental associations and mechanisms controlling the interannual variability of precipitation in each region be examined separately, and combined to gain understanding of the variability over India as a whole.

Acknowledgments. This publication is funded by the Joint Institute for the Study of the Atmosphere and Ocean (JISAO), under NOAA Cooperative Agreement No. NA17RJ11232, Contribution #943, by NOAA (OAR HQ and OGP) through UW/PMEL Hayes center, and by NASA's physical oceanography program. Analysis and graphics done using freeware package Ferret (http://ferret.wrc.noaa.gov/). PMEL cont. 2518. The global gridded rain gauge precipitation data (Version 1.0) is constructed and supplied by Dr Mike Hulme at the Climatic Research Unit, University of East Anglia, Norwich, UK; whose work has been supported by the UK Department of the Environment, Transport and the Regions (Contract EPG 1/1/85). Indian sub-divisional rainfall is made available by Dr. B. Parthasarathy, Indian Institute of Tropical Meteorology, Pune 411 008, India. Helpful comments, discussion and suggestions from N. Bond, J. Callahan, K. McHugh, and S. Ilcane.

REFERENCES

Alapaty, K., S. Raman, U.C. Mohanty, and R.V. Madala, Sensibility of Monsoon Circulations to Changes in Sea Surface Temperatures. *Atmos. Environ.*, 29(16), 2139-2155, 1995.

Cadet, D.L., and S. Greco, Water vapor transport over the Indian Ocean during the 1979 summer monsoon, Pt. 1, Water vapor fluxes. *Mon. Wea. Review*, 115(2), 653-663, 1987.a.

Cadet, D.L., and S. Greco, Water vapor transport over the Indian Ocean during the 1979 summer monsoon, Pt. 2, Water vapor budgets. *Mon. Wea. Review*, 115(10), 2358-2366, 1987.b.

Clark, C.O., J.E. Cole, and P.J. Webster, Indian Ocean SST and Indian Summer Rainfall: Predictive Relationships and Their Decadal Variability. *J. Climate*, 13, 2503-2519, 2000.

Druyan, L.M., J.R. Miller, and G.L. Russell, Atmospheric General Circulation Model Simulations With an Interactive Ocean: Effects of Sea Surface Temperature Anomalies in the Arabian Sea. *Atmos.-Ocean*, 21(1), 94-106, 1983.

Findlater, J., Interhemispheric transport of air in the lower troposphere over the western Indian Ocean. *Q. J. R. Meteorol. Soc.*, 95, 400-403, 1969.

Gadgil, S., Yadumani, and N.V. Joshi, Coherent Rainfall Zones of the Indian Region. *International J. Climatology*, 13, 547-566, 1993.

Goswami, B.N., V. Krishnamurthy, and H. Annamalai, A broad-scale circulation index for interannual variability of the Indian summer monsoon. *Q.J.R. Meteorol. Soc.*, 125, 611-633, 1999.

Harrison, D.E., and G.A. Vecchi, January 1999 Indian Ocean cooling event. *Geophys. Res. Lett.*, 28(19), 3717–3720, 2001.

Hastenrath, S., On the Prediction of India Monsoon Rainfall Anomalies. *J. Climate and Applied Meteorol.*, 26, 847-857, 1987.

Hulme, M., A 1951-80 global land precipitation climatology for the evaluation of General Circulation Models, *Climate Dynamics*, 7, 57-72, 1992.

Hulme, M., Validation of large-scale precipitation fields in General Circulation Models pp.387-406 in, *Global precipitations and climate change* (eds.) Desbois, M. and Desalmand, F., NATO ASI Series, Springer-Verlag, Berlin, 466pp, 1994.

Hulme, M., T.J. Osborn, and T.C. Johns, Precipitation sensitivity to global warming: Comparison of observations with HadCM2 simulations. *Geophys. Res. Letts.*, 25, 3379-3382, 1998.

Iyengar, R.N., and P. Basak, Regionalization of Indian Monsoon Rainfall and Long-term Variability Signals. *International J. Climatology*, 14, 1095-1114, 1994.

Joseph, P.V., and P.V. Pillai, Air-Sea interaction on a seasonal scale over north Indian Ocean – Part I: Inter-annual variations of sea surface temperature and the Indian summer monsoon rainfall. *Mausam*, 35(3), 323-330, 1984.

Kershaw, R., The effect of a sea surface temperature anomaly on a prediction of the onset of the south-west monsoon over Indian. *Q. J. R. Meteorol. Soc.*, 114, 325-345, 1988.

Krishnamurthy, V., and B.N. Goswami, Indian Monsoon-ENSO Relationship on Interdecadal Timescales. *J. Climate*, 13, 579-595, 2000.

Mooley, D.A., B. Parthasarathy, N.A. Sontakke, and A.A. Munot, Annual Rain-Water over India, its Variability and Impact on the Economy. *J. Climatology*, 1, 167-186, 1981.

Mooley, D.A., and B. Parthasarathy, Indian Summer Monsoon

and El Nino. *Pageoph*, 121(2), 339-352, 1983.

Mooley, D.A., and B. Parthasarathy, Indian Summer Monsoon and the East Equatorial Pacific Sea Surface Temperature. *Atmosphere-Ocean*, 22(1), 23-35, 1984.

Murakami, M., Analysis of Summer Monsoon Fluctuations over India. *J. Meteorol. Soc. Japan*, 54(1), 15-31, 1976.

Nicholls, N., All-Indian Summer Monsoon Rainfall and Sea Surface Temperatures around Northern Australia and Indonesia. *J. Climate*, 8, 1463-1467, 1995.

Parthasarathy, B., Interannual and long-term variability of Indian summer monsoon rainfall. *Proc. Indian Acad. Sci.*, 93(4), 371-385, 1984.

Parthasarathy, B., and G.B. Pant, The spatial and temporal relationships between Indian summer rainfall and the Southern Oscillation. *Tellus*, 36A, 269-277, 1984.

Parthasarathy, B., A.A. Munot, and D.R. Kothawale, Regression Model for Estimation of Indian Foodgrain Production from Summer Monsoon Rainfall. *Agricultural and Forest Meteorol.*, 42, 167-182, 1988.a.

Parthasarathy, B., H.F. Diaz, and J.K. Eischeid, Prediction of All-India Summer Monsoon Rainfall With Regional and Large-Scale Parameters. *J. Geophys. Res.*, 93(D5), 5341-5350, 1988.b.

Parthasarathy, B., K. Rupa Kumar, and D.R. Kothawale, Indian summer monsoon rainfall indices: 1871-1990. *Meteorol. Mag.*, 121, 174-186, 1991.

Parthasarathy, B., A.A. Munot, and D.R. Kothawale, Monthly and seasonal rainfall series for All-India homogeneous regions and meteorological subdivisions: 1871-1994. *Contributions from Indian Institute of Tropical Meteorology*, Research Report RR-065, Pune 411 008 India, August 1995

Premkumar, K., M. Ravichandran, S. R. Kalsi, D. Sengupta, and S. Gadgil, First results from a new observational system over the Indian seas. *Curr. Sci.*, 78, 323–330, 2000.

Rakhecha, P.R., and P.R. Pisharoty, Heavy rainfall during monsoon season: Point and spatial distribution. *Curr. Sci.*, 71(3), 179-186, 1996.

Ramesh Kumar, M.R., and J.S. Sastry, Relationships Between Sea Surface Temperature, Southern Oscillation, Position of the 500 mb Ridge along 75°E in April and the Indian Monsoon Rainfall. *J. Meteorol. Soc. Japan*, 68(6), 741-745, 1990.

Rao, K.G., and B.N. Goswami, Interannual Variations in Sea Surface Temperature of the Arabian Sea and the Indian Monsoon: A New Perspective. *Mon. Wea. Rev.*, 116, 558-568, 1988.

Rasmusson, E.M., and T.H. Carpenter, The relationship between eastern equatorial Pacific sea surface temperature and rainfall over India and Sri Lanka. *Mon. Wea. Rev.*, 11, 517-528, 1983.

Reynolds, R.W., and T.M. Smith, Improved global sea surface temperature analyses using optimum interpolation. *J. Climate*, 7, 1195-1202, 1994.

Reynolds, R.W, N.A. Rayner, T.M. Smith, D.C. Stokes, W. Wang, An Improved In Situ and Satellite SST Analysis for Climate. *J. Clim.*, 15(13), 1609–1625, 2002.

Sadhuram, Y., Predicting monsoon rainfall and pressure indices from sea surface temperature. *Curr. Sci.*, 72(3), 166-168, 1997.

Saha, K., Zonal Anomaly of sea surface temperature in equatorial Indian Ocean and its possible effect upon monsoon circulation. *Tellus*, XXII, 403-409, 1970.a.

Saha, K., Air and water vapor transport across the equator in western Indian Ocean during northern summer. *Tellus*, XXII, 681-687, 1970.b.

Saha, K., Some aspects of the Arabian Sea summer monsoon. *Tellus*, XXVI, 464-476, 1974.

Saha, K.R., and S.N. Bavadekar, Moisture flux across the west coast of India and rainfall during the southwest monsoon. *Q.J.R. Meteorol. Soc.*, 103(436), 370-374, 1977.

Sengupta, D., and M. Ravichandran, Oscillations of Bay of Bengal sea surface temperature during the 1998 summer monsoon. *Geophys. Res. Lett.*, 28, 2033–2036, 2001.

Shukla, J., Effect of Arabian Sea-Surface Temperature Anomaly on Indian Summer Monsoon: A Numerical Experiment with the GFDL Model. *J. Atmos. Sci.*, 32, 503-511, 1975.

Shukla, J., and B.M. Misra, Relationships Between Sea Surface Temperature and Wind Speed Over the Central Arabian Sea, and Monsoon Rainfall Over India. *Mon. Wea. Rev.*, 105, 998-1002, 1977.

Shukla, J., Interannual variability of monsoons, in "Monsoons", edited by J.S. Fein and P.L. Stephens, 399-464. John Wiley and Sons, 1987.

Subbaramayya, I., and C.V. Naidu, Spatial Variations and Trends in the Indian Monsoon Rainfall. *International J. of Climatology*, 12, 597-609, 1992.

Torrence, C., and P.J. Webster, Interdecadal Changes in the ENSO-Monsoon System. *J. Climate*, 12, 2679-2690, 1999.

Vecchi, G.A., and D.E. Harrison. Monsoon Breaks and subseasonal sea surface temperature variability in the Bay of Bengal. *J. Climate*, 15(12), 1485-1493, 2002.

Webster, P.J. *et al.*, Monsoons: Processes, predictability and prospects for prediction. *J. Geophys. Res. (TOGA Special Issue)*, 103, 14,451-14,510, 1998.

Xie, P. and P.A. Arkin, Analyses of Global Monthly Precipitation Using Gauge Observations, Satellite Estimates, and Numerical Model Predictions. *J. Clim*, 9, 840 -858, 1996.

Xie, P., and P.A. Arkin, Global precipitation: a 17-year monthly analysis based on gauge observations, satellite estimates, and numerical model outputs. *Bull. Amer. Meteorol. Soc.*, 78(11), 2539-2558, 1997.

Yu, J., and J. Slingo, The asian summer monsoon and ENSO. *Q.J.R. Meteorol. Soc.*, 121, 1133-1168, 1995.

D.E. Harrison, Pacific Marine Environmental Laboratory, NOAA, 7600 Sand Point Way NE, Seattle, WA 98115 (e-mail: D.E.Harrison@noaa.gov)

Gabriel A. Vecchi, Joint Institute for the Study of Atmosphere and Ocean, Box 354235, University of Washington Seattle, WA 98195-4235 U.S.A. (e-mail: vecchi@atmos.washington.edu)

FIGURE CAPTIONS

Figure 1. Filled maps of the (a) mean precipitation over June-September, (b) standard deviation of the June-September monthly-mean precipitation anomaly. Shaded map (c) of the standard deviation of monthly-mean June-September precipitation anomaly, indicating the actual grid-cells used in the computation of the indices. The figures are based on the 1979-2001 CMAP precipitation data. Units are mm/day.

Figure 1. Filled maps of the (a) mean precipitation over June-September, (b) standard deviation of the June-September monthly-mean precipitation anomaly. Shaded map (c) of the standard deviation of monthly-mean June-September precipitation anomaly, indicating the actual grid-cells used in the computation of the indices. The figures are based on the 1979-2001 CMAP precipitation data. Units are mm/day.

Figure 2. Shaded maps of the correlation coefficient of the mean June-September precipitation anomaly in each land grid-cell with mean June-September precipitation anomaly at (a) (76.25°E, 13.75°N) and (b) (81.25°E, 23.75°N). Correlations are based on the 1979-2001 CMAP data, only values greater than 0.4 are shaded (representing statistical significance at the 95% level). In each panel the areas that are used to define the regional indices are indicated by black boxes. Notice that the precipitation anomalies are correlated only locally within each region.

Figure 2. Shaded maps of the correlation coefficient of the mean June-September precipitation anomaly in each land grid-cell with mean June-September precipitation anomaly at (a) (76.25°E, 13.75°N) and (b) (81.25°E, 23.75°N). Correlations are based on the 1979-2001 CMAP data, only values greater than 0.4 are shaded (representing statistical significance at the 95% level). In each panel the areas that are used to define the regional indices are indicated by black boxes. Notice that the precipitation anomalies are correlated only locally within each region.

Figure 3. (a) Time series of the mean June-September precipitation anomaly over the two regions: Ganges-Mahanadi Basin (black line) and Western Ghats (gray line). (b) Time series of the mean June-September precipitation anomaly over All-India (black line) and the average of GBI and WGI. Units are mm/day. Correlation coefficients between the time series are indicated in the panels.

Figure 3. (a) Time series of the mean June-September precipitation anomaly over the two regions: Ganges-Mahanadi Basin (black line) and Western Ghats (gray line). (b) Time series of the mean June-September precipitation anomaly over All-India (black line) and the average of GBI and WGI. Units are mm/day. Correlation coefficients between the time series are indicated in the panels.

Figure 4. Correlations of JJAS-mean GBI (a)-(d) and WGI (e)-(h) with Indian Ocean SSTA in (a),(e) June-July, (b),(f) March-April, (c),(g) December-January, (d),(h) September October. Only those correlations whose amplitude exceeds 0.4 are shown (representing statistical significance at the 92.5% level), and only over those regions where the local SSTA standard deviation (SSTA first averaged over the months to be correlated) exceeds 0.3°C. Correlations are computed over the period 1982-2001.

Figure 4. Correlations of JJAS-mean GBI (a)-(d) and WGI (e)-(h) with Indian Ocean SSTA in (a),(e) June-July, (b),(f) March-April, (c),(g) December-January, (d),(h) September October. Only those correlations whose amplitude exceeds 0.4 are shown (representing statistical significance at the 92.5% level), and only over those regions where the local SSTA standard deviation (SSTA first averaged over the months to be correlated) exceeds 0.3°C. Correlations are computed over the period 1982-2001.

Figure 5. Scatter plots of Ganges-Mahanadi Basin Precipitation anomaly vs. SSTA averaged over (a) June-July, 95°E-110°E, 15°S-5°S; (b) December-January, 65°E-85°E, 25°S-20°S; (c) September-October, 60°E-90°E, 30°S-20°S. These are the months/regions with which GBI exhibits large-scale SSTA correlations. Indicated in each panel is the correlation coefficient between the two quantities. Notice that the correlation with June-July 1994 arises from a single extreme point.

Figure 5. Scatter plots of Ganges-Mahanadi Basin Precipitation anomaly vs. SSTA averaged over (a) June-July, 95°E-110°E, 15°S-5°S; (b) December-January, 65°E-85°E, 25°S-20°S; (c) September-October, 60°E-90°E, 30°S-20°S. These are the months/regions with which GBI exhibits large-scale SSTA correlations. Indicated in each panel is the correlation coefficient between the two quantities. Notice that the correlation with June-July 1994 arises from a single extreme point.

Figure 6. Scatter plots of Western Ghats Precipitation anomaly vs. SSTA averaged over (a) June-July, 50°E-60°E, 5°N-10°N; (b) March-April, 65°E-80°E, 20°S-10°S; (c) September-October, 55°E-65°E, 15°S-5°S. These are the months/regions with which GBI exhibits large-scale SSTA correlations. Indicated in each panel is the correlation coefficient between the two quantities. Notice that the correlations are all relatively robust.

Figure 6. Scatter plots of Western Ghats Precipitation anomaly vs. SSTA averaged over (a) June-July, 50°E-60°E, 5°N-10°N; (b) March-April, 65°E-80°E, 20°S-10°S; (c) September-October, 55°E-65°E, 15°S-5°S. These are the months/regions with which GBI exhibits large-scale SSTA correlations. Indicated in each panel is the correlation coefficient between the two quantities. Notice that the correlations are all relatively robust.

Figure 7. As in Figure 4, but for AIRI. Only those correlations whose amplitude exceeds 0.4 are shaded, and only over those regions where the local SSTA standard deviation exceeds 0.3°C. Contours indicate values where the amplitude of the correlation is less that 0.4, contour interval in non-shaded regions is 0.2, in shaded regions it is 0.1. Correlations are computed over the period 1982-2001.

Figure 7. As in Figure 4, but for AIRI. Only those correlations whose amplitude exceeds 0.4 are shaded, and only over those regions where the local SSTA standard deviation exceeds 0.3°C. Contours indicate values where the amplitude of the correlation is less that 0.4, contour interval in non-shaded regions is 0.2, in shaded regions it is 0.1. Correlations are computed over the period 1982-2001.

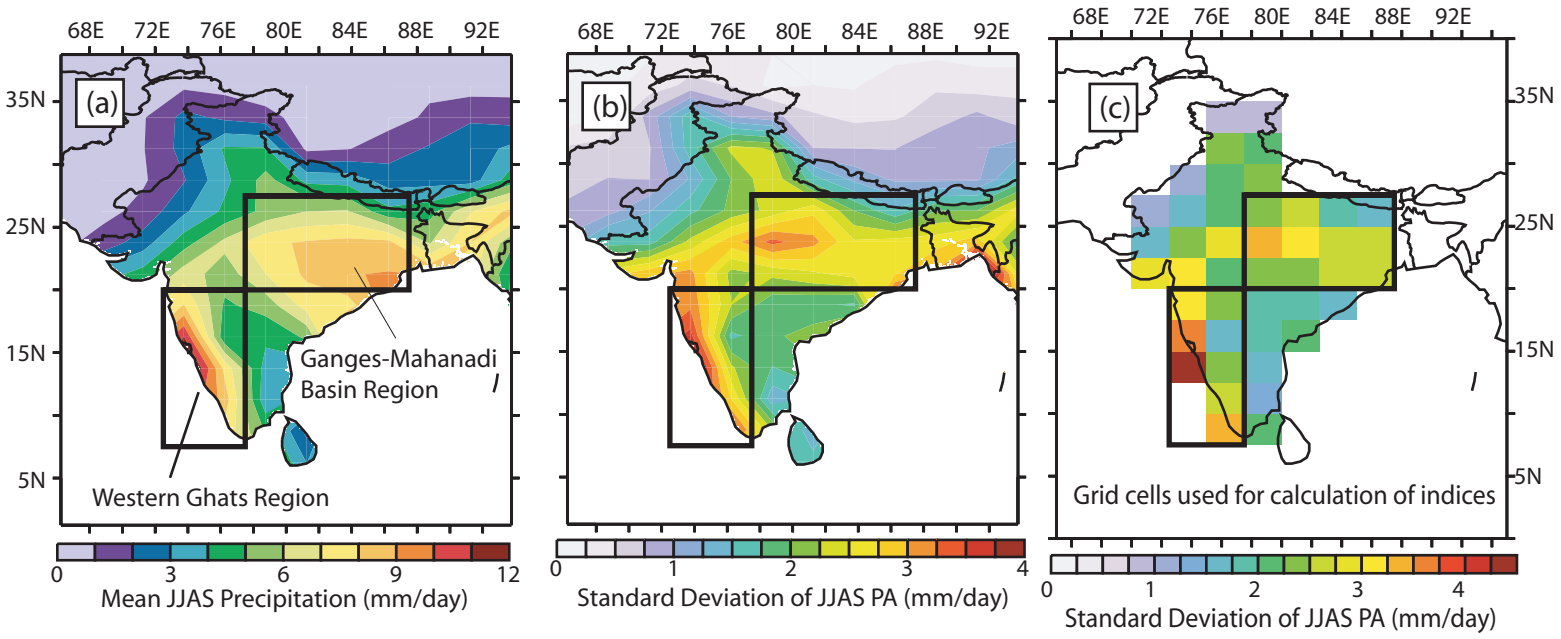

Figure 1: Filled maps of the (a) mean precipitation over June-September, (b) standard deviation of the June-September monthly-mean precipitation anomaly. Shaded map (c) of the standard deviation of monthly-mean June-September precipitation anomaly, indicating the actual grid-cells used in the computation of the indices. The figures are based on the 1979-2001 CMAP precipitation data. Units are mm/day.

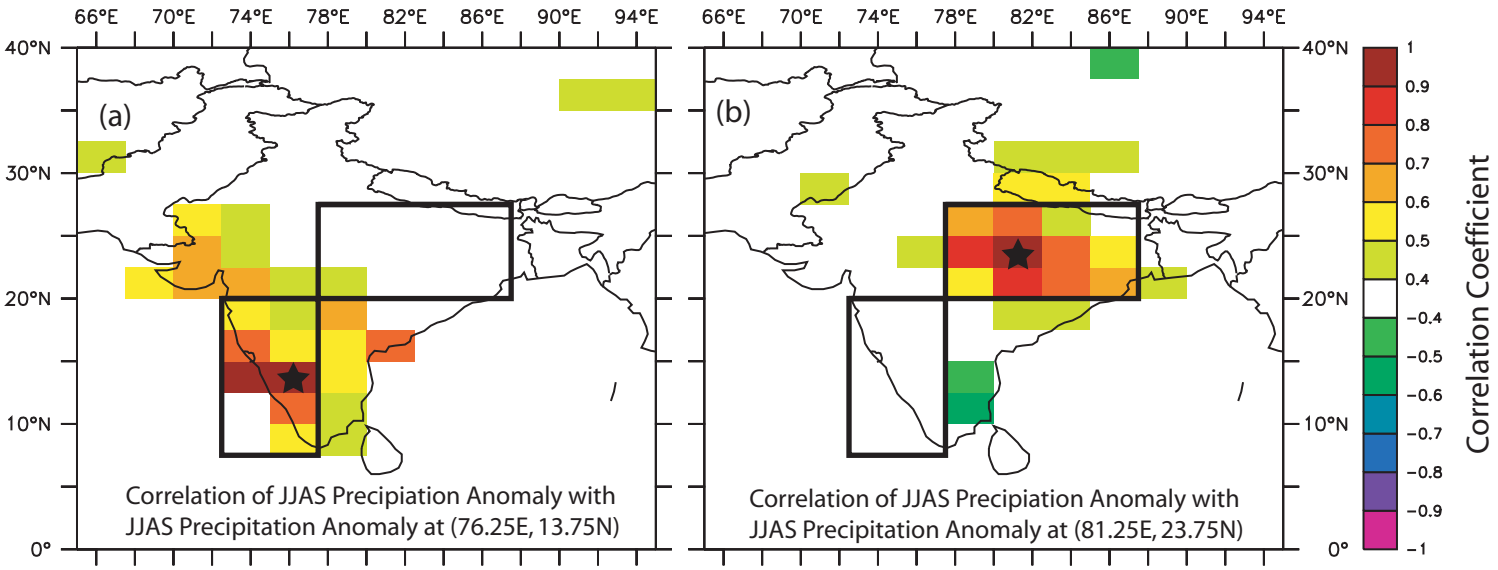

Figure 2: Shaded maps of the correlation coefficient of the mean June-September precipitation anomaly in each land grid-cell with mean June-September precipitation anomaly at (a) (76.25°E, 13.75°N) and (b) (81.25°E, 23.75°N). Correlations are based on the 1979-2001 CMAP data, only values greater than 0.4 are shaded. In each panel the areas that are used to define the regional indices are indicated by black boxes. Notice that the precipitation anomalies are correlated only locally within each region.

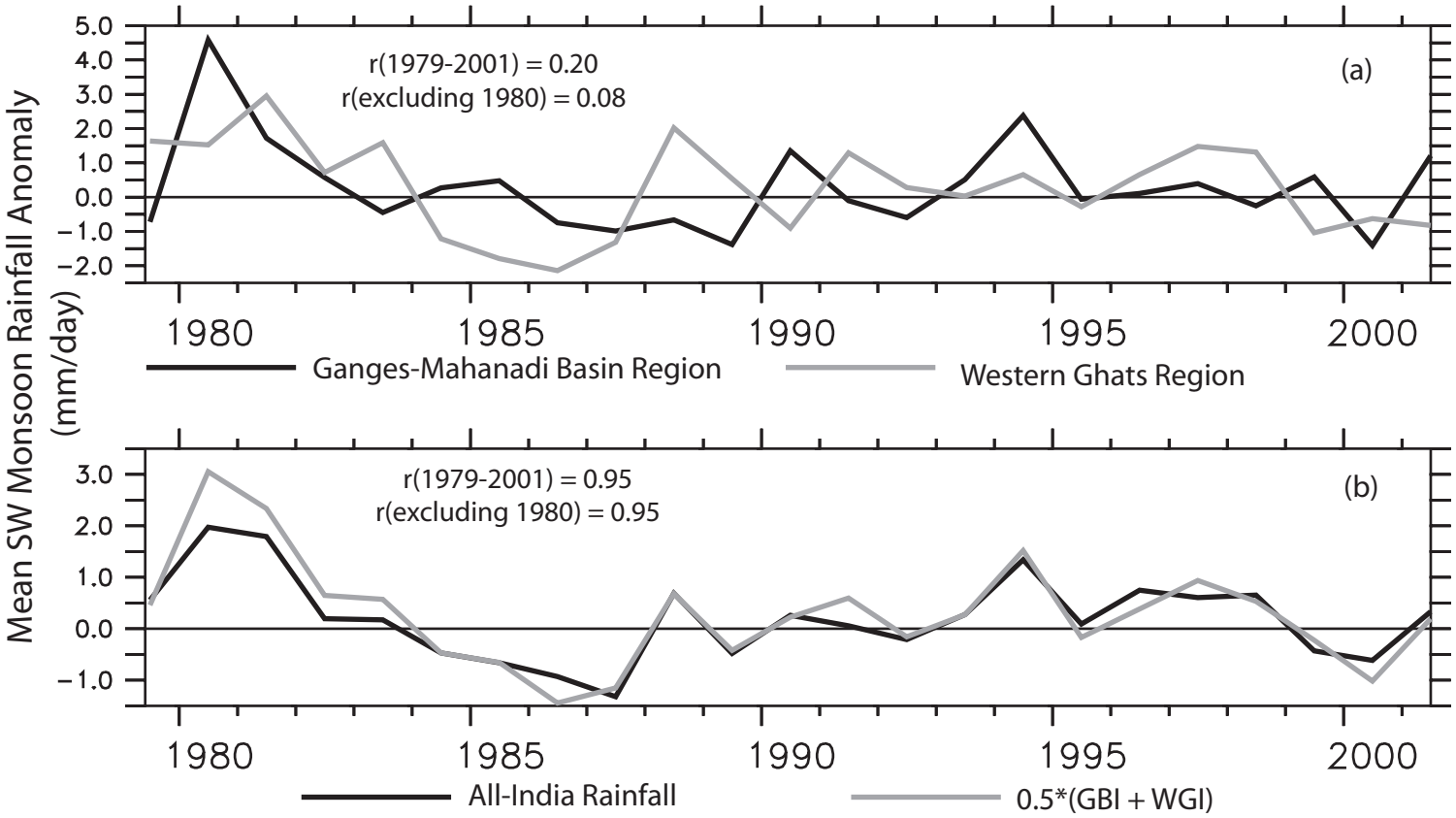

Figure 3: (a) Time series of the mean June-September precipitation anomaly over the two regions: Ganges-Mahanadi Basin (black line) and Western Ghats (gray line). (b) Time series of the mean June-September precipitation anomaly over All-India (black line) and the average of GBI and WGI. Units are mm/day. Correlation coefficients between the time series are indicated in the panels.

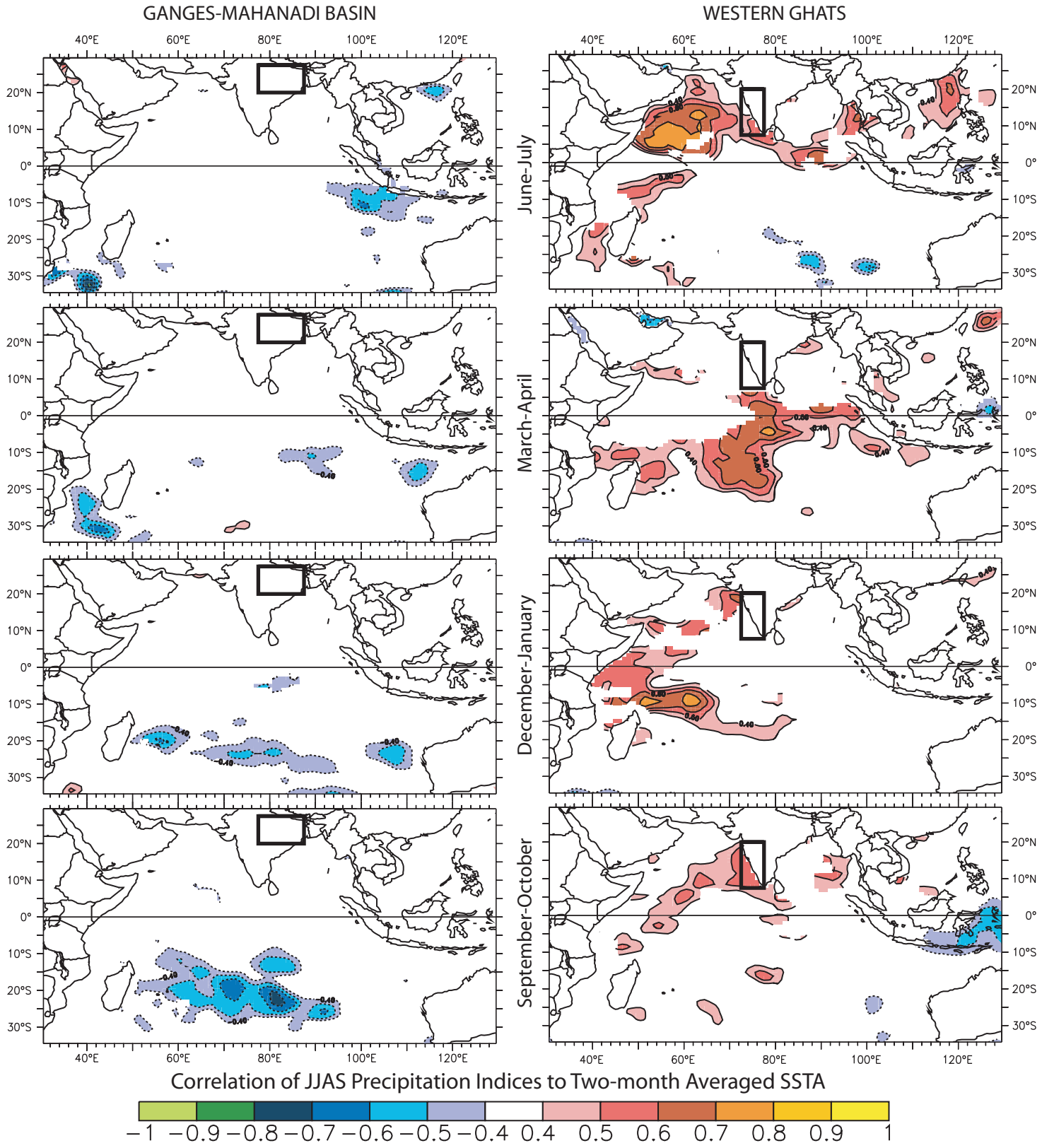

Figure 4: Correlations of JJAS-mean GBI (a)-(d) and WGI (e)-(h) with Indian Ocean SSTA in (a),(e) June-July, (b),(f) March-April, (c),(g) December-January, (d),(h) September October. Only those correlations whose amplitude exceeds 0.4 are shown, and only over those regions where the local SSTA standard deviation (SSTA first averaged over the months to be correlated) exceeds 0.3°C. Correlations are computed over the period 1982-2001.

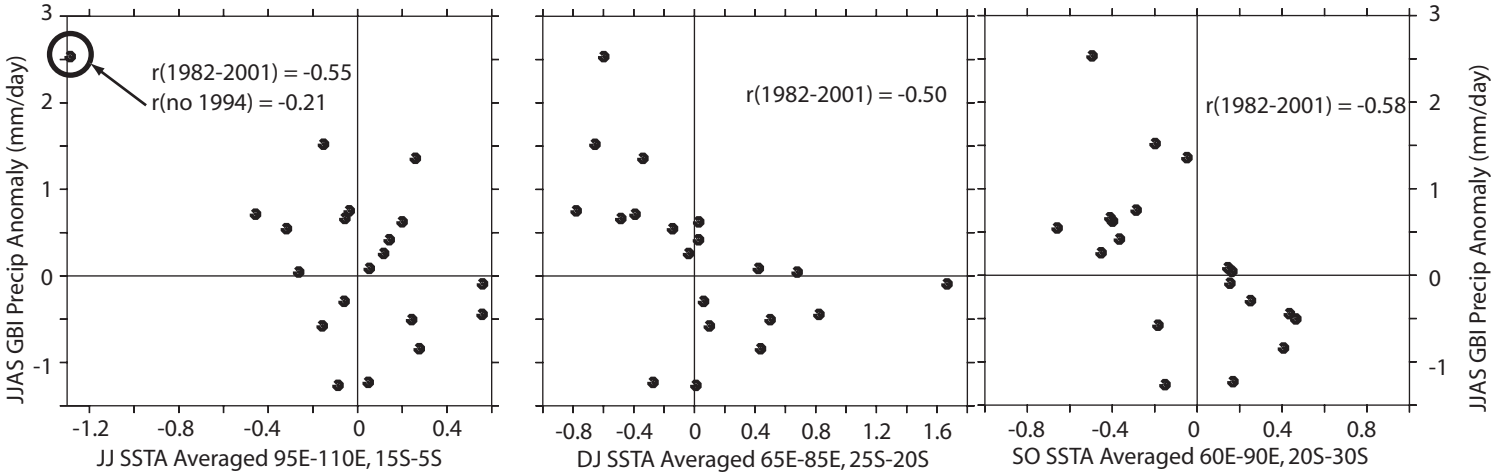

Figure 5: Scatter plots of GBI Precipitation anomaly vs. SSTA averaged over (a) June-July, 95°E-110°E, 15°S-5°S; (b) December-January, 65°E-85°E, 25°S-20°S; (c) September-October, 60°E-90°E, 30°S-20°S. These are the months/regions with which GBI exhibits large-scale SSTA correlations. Indicated in each panel is the correlation coefficient between the two quantities. Notice that the correlation with June-July 1994 arises from a single extreme point.

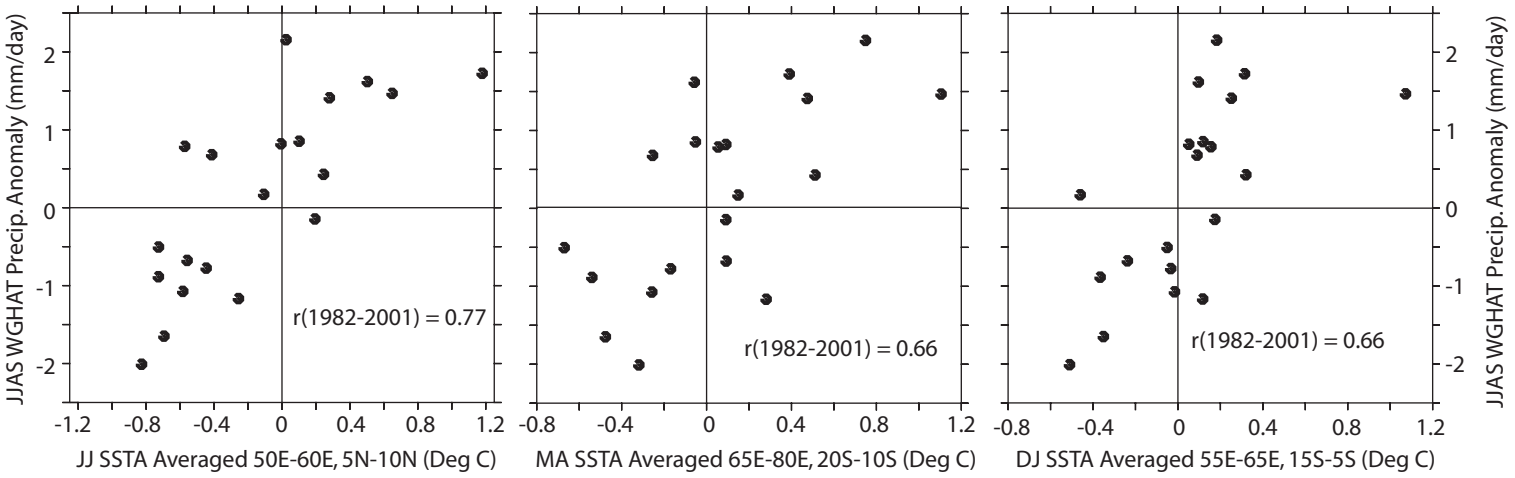

Figure 6: Scatter plots of Western Ghats Precipitation anomaly vs. SSTA averaged over (a) June-July, 50°E-60°E, 5°N-10°N; (b) March-April, 65°E-80°E, 20°S-10°S; (c) September-October, 55°E-65°E, 15°S-5°S. These are the months/regions with which GBI exhibits large-scale SSTA correlations. Indicated in each panel is the correlation coefficient between the two quantities. Notice that the correlation are all relatively robust.

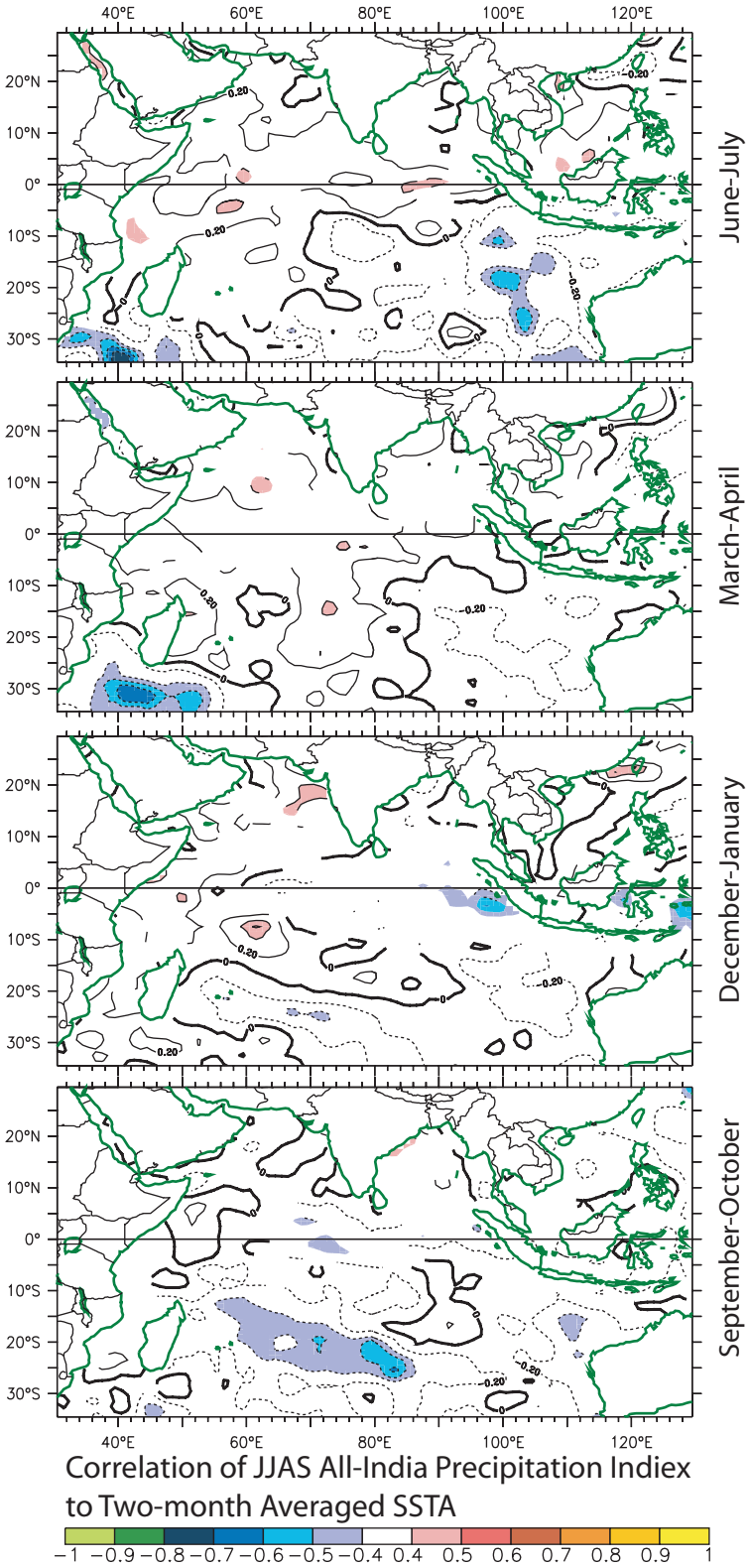

Figure 7: As in Figure 4, but for AIRI. Only those correlations whose amplitude exceeds 0.4 are shaded, and only over those regions where the local SSTA standard deviation exceeds 0.3°C. Contours indicate values where the amplitude of the correlation is less that 0.4, contour interval in non-shaded regions is 0.2, in shaded regions it is 0.1. Correlations are computed over the period 1982-2001.